D, *E*, and *F* layers in the daytime at high-latitude terminator ionosphere of Mars: Comparison with Earth's ionosphere using COSMIC data

S. A. Haider,[1,2] M. A. Abdu,[1] I. S. Batista,[1] J. H. Sobral,[1] Xiaoli Luan,[3] Esa Kallio,[4] W. C. Maguire,[5] M. I. Verigin,[6] and V. Singh[7]

Received 28 August 2008; revised 26 November 2008; accepted 12 January 2009; published 21 March 2009.

[1] We report the first model result for ion production rates and densities of positive ions, negative ions, and electrons in the dayside Martian ionosphere from 0 to 220 km. These calculations are made at solar zenith angle 77° for low solar activity periods. The calculated electron density is compared with the radio occultation measurements made by Mars Global Surveyor (MGS) and Mars 4/5 on Mars and by Constellation Observing System for Meteorology, Ionosphere and Climate (COSMIC) on Earth. Our calculation suggests that the daytime ionosphere of Mars can be divided into *D*, *E*, and *F* layers at altitude ranges ~25–35 km, ~100–112 km, and ~125–145 km with the concentrations 7×10^1 cm^{-3}, 2.4×10^4 cm^{-3}, and 8.4×10^4 cm^{-3} owing to the impact of galactic cosmic rays, X rays (10–90 Å), and solar EUV (90–1026 Å) radiations, respectively. The water cluster ions $H_3O^+(H_2O)_n$, $NO_2^-(H_2O)_n$, and $CO_3^-(H_2O)_n$ are dominated in the *D* region, while NO^+, CO_2^+, and O_2^+ are major ions in the *E* and *F* regions. The calculated *E* and *F* peak heights are in good agreement with MGS observation. The value of *D* peak density is lowered by 1 and 2 orders of magnitude from the measurements on Mars and Earth, respectively. The height of *F* layer peak is lower by factor of 1.8 in the Martian ionosphere as compared to that observed in the ionosphere of Earth. *E* regions are created at nearly the same heights in the ionospheres of both planets, but the layer thickness is considerably less on Mars than on Earth. This implies that solar EUV energy is deposited within smaller-altitude range in the upper ionosphere of Mars as compared to the corresponding altitude range in the upper ionosphere of Earth.

Citation: Haider, S. A., M. A. Abdu, I. S. Batista, J. H. Sobral, X. Luan, E. Kallio, W. C. Maguire, M. I. Verigin, and V. Singh (2009), *D*, *E*, and *F* layers in the daytime at high-latitude terminator ionosphere of Mars: Comparison with Earth's ionosphere using COSMIC data, *J. Geophys. Res.*, *114*, A03311, doi:10.1029/2008JA013709.

1. Introduction

[2] The ionosphere of Earth is divided into *D*, *E*, and *F* regions [cf. *Richmond*, 1987; *Kelley*, 1989]. The *F* region is formed mainly owing to photoionization of neutral atoms/molecules by EUV radiation (800–1026 Å) and, at higher latitudes, also by the precipitation of energetic charged particles. The major gases N_2, O_2, and O are ionized by these radiations. The primary ions are produced as N_2^+, O_2^+, N^+ and O^+. The maximum ionization in the *F* region occurs at altitude ~250–300 km. This region has dense layer of O^+ ions that sometimes get split into two distinct F_1 and F_2 layers [cf. *Fox*, 2005]. The *E* region is produced by X-ray (10–100 Å) radiation. The ion composition measurements show that O_2^+ and NO^+ are the major ions in the *E* region with N_2^+ and O^+ as minor ions [*Brasseur and Solomon*, 2005]. The *E* region represents maximum ionization at altitude ~90–140 km. Within *E* region, local enhancements and irregularities in electron density known as sporadic *E* are observed. At midlatitude sporadic *E* is formed from layering of metallic ions. The equatorial sporadic *E* on the other hand is due to small-scale irregularities resulting from the plasma instabilities occurring in the electrojet region [*Rishbeth and Garriott*, 1969; *Hargreaves*, 1992]. The formation of *D* region is the result of the following ionization sources: (1) solar Lyman α (1216 Å) ionizing the minor constituent NO, (2) solar X rays ($\lambda < 8$ Å) ionizing N_2 and O_2, (3) galactic cosmic rays ionizing all atmospheric constituents and (4) photoionization of the metastable $O_2(^1\Delta_g)$ by solar UV radiation ($\lambda < 1118$ Å). The ions O_2^+ and NO^+ produced by these processes are converted into $H_3O^+(H_2O)_n$ mainly by three body reactions

[1]Department of Aeronomy, Instituto Nacional de Pesquisas Espaciais, Sao Paulo, Brazil.
[2]Now at Space and Atmospheric Sciences, Physical Research Laboratory, Ahmedabad, India.
[3]National Center for Atmospheric Research, Boulder, Colorado, USA.
[4]Finnish Meteorological Institute, Helsinki, Finland.
[5]Solar System Exploration Division, NASA Goddard Space Flight Centre, Greenbelt, Maryland, USA.
[6]Space Research Institute, Russian Academy of Sciences, Moscow, Russia.
[7]Department of Electronics for Automation, University of Brescia, Brescia, Italy.

0148-0227/09/2008JA013709$09.00

[*Banks and Kockarts*, 1973; *Schunk and Nagy*, 2000]. This layer occurs at altitude region ~60–90 km.

[3] The upper ionosphere of Mars has been explored during encounters of Mariner 6, 7, and 9 [*Fjeldbo et al.*, 1970; *Kliore et al.*, 1972], Mars 2, 3, 4, 6, and 7 [*Rasool and Stewart*, 1971; *Vasiliev et al.*, 1975], Viking 1 and 2 [*Fjeldbo et al.*, 1977], and recently by Mars Global Surveyor (MGS) [*Acuna et al.*, 1998; *Ness et al.*, 2000] and Mars Express [*Gurnett et al.*, 2005]. These measurements have shown two ionization peaks in most of the electron density profiles at about 137 km and 110 km on the dayside ionosphere of Mars. The values of the first and the second peaks were observed to be $\sim 8.6 \times 10^4$ cm^{-3} and $2.5–4.0 \times 10^4$ cm^{-3}, respectively. We have reproduced these ionization peaks as owing to impact of solar EUV (90–1025.7 Å) and X-ray (10–90 Å) photons, respectively, with the upper atmosphere of Mars [*Haider et al.*, 2002, 2006]. *Ma et al.* [2004], *Ma and Nagy* [2007], and *Duru et al.* [2008] have also studied upper ionosphere of Mars using three dimensional models. Mars possesses a disappearing ionosphere at most of the nighttime, while a major peak is observed at altitude ~125–145 km when it appears [*Zhang et al.*, 1990]. In spite of relatively large number of measurements and models concerning Mars upper atmosphere, no special attention has been paid to the ionosphere of Mars below 80 km.

[4] The first theoretical study of the lower ionosphere of Mars was carried out by *Whitten et al.* [1971]. They considered ionization by cosmic rays and solar radiation on the dayside ionosphere of Mars. Later, *Molina-Cuberos et al.* [2002] calculated electron density in the daytime lower ionosphere of Mars. Recently we have modeled the electron density in the nighttime ionosphere of Mars, owing to absorption of solar wind electron and galactic cosmic rays, between altitudes 0 and 220 km [*Haider et al.*, 2007]. *F* and *D* layers are produced in the nighttime ionosphere at altitudes ~130–140 km and ~30 km, respectively. *E* layer is not clearly visible. In the *D* region ionosphere, the densities of hydronium ions ($H_3O^+(H_2O)_n$ for n = 1,2,3 and 4) and electron are higher than the daytime by factor of ~2. This difference between daytime and nighttime model ionosphere is mainly due to use of different chemistry in the two model calculations. The photodissociation and electron photodetachment reactions are not used in the nighttime chemical model. These reactions reduce ion densities in the daytime ionosphere at low-altitude region. The neutral densities are not significantly different in the daytime and nighttime model atmospheres. We do not know what fraction of galactic cosmic rays actually precipitate into dayside and nightside atmosphere of Mars. Therefore, we have used same energy flux of galactic cosmic rays in both model calculations.

[5] This model is now extended to study the different ion layers in the dayside ionosphere over Mars. In this model we have used three sources of ionizations: solar EUV, X rays, and galactic cosmic rays. This model couples ion-neutral and electron-neutral collisions, photodissociation of positive and negative ions, electron attachment, ion-ion, ion-electron recombination processes through 133 chemical reactions. The calculated electron density is compared with the observations made by MGS and Mars 4/5 in the Mars' ionosphere and by Constellation Observing System for Meteorology, Ionosphere and Climate (COSMIC) satellites in Earth's ionosphere.

2. Objective

[6] The only planet for which we have direct observations of the details of *D*, *E*, and *F* layers is Earth. Mars has neither in situ nor remote sensing measurements in the low-altitude daytime ionosphere. However, nighttime radio occultation measurements have provided clues for presence or absence of low-altitude ionosphere together with upper ionosphere over Mars [*Savich and Samovol*, 1976; *Zhang et al.*, 1990]. An understanding of the complete ionosphere of Mars can only be developed by using theoretical models. For the first time we have developed a model, which provides simultaneously the *D*, *E*, and *F* layers of dayside ionosphere of Mars at altitudes ~25–35 km, 100–112 km and ~125–145 km with the electron concentrations of $\sim 7 \times 10^1$ cm^{-3}, $\sim 2.4 \times 10^4$ cm^{-3} and $\sim 8.4 \times 10^4$ cm^{-3}, respectively. These densities are produced owing to impact of galactic cosmic rays, X rays (10–90 Å) and solar EUV (90–1026 Å) radiations, respectively. This model calculates ion production rates and densities of positive ions, negative ions and electron at solar zenith angle 77° in the ionosphere over Mars. In the chemistry of *D* region hydrated hydronium ions $H_3O^+(H_2O)_n$ for n = 1,2,3 and 4 and water clusters $NO_2^-(H_2O)_n$ and $CO_3^-(H_2O)_n$ for n = 1 and 2 dominate, while NO^+, CO_2^+, and O_2^+ are the major ions in *E* and *F* regions. The *D* region chemistry which is more complex than chemistry of the *E* and *F* regions has not been elucidated fully. Nevertheless, there has been success in modeling the *D* region. As expected the height and density of the *F* layer peak are lower in the Martian ionosphere than Earth's ionosphere by factors of ~1.8 and ~3, respectively. *E* layers in the ionosphere of Earth and Mars are formed at nearly same height interval between 90 km and 115 km. The calculated electron density in the *D* region is smaller by 1 and 2 orders of magnitude than those observed in the ionospheres of Mars and Earth, respectively. The formation of present chemical model is purely a sequence of algebraic expressions, which yield solutions after sufficient iterations for electron concentration and all the individual ions currently in the model, 22 positive ions and 13 negative ions. Because of the fact that transport time is several orders of magnitude higher than chemical life time at altitude $\leq$200 km, we have neglected transport of ions in the present calculation.

3. Input Data

[7] Viking Landers carried neutral mass spectrometer that measured daytime densities at Martian midlatitude during summer of minimum solar activity. The densities of CO_2, N_2, O_2, CO, NO and Ar are taken from this measurement [cf. *Nier and McElroy*, 1977; *Nier et al.*, 1976; *Biemann et al.*, 1976; *Owen et al.*, 1977]. O_3 has been obtained from the observation with UV spectrometer onboard Mariner 7 [*Barth and Hord*, 1971]. Modeling has provided better knowledge of neutral compositions and structure compared to what is known from the measurements. *Rodrigo et al.* [1990] and *Nair et al.* [1994] have modeled the atmospheric constituents CO_2, N_2, Ar, O_2, CO, H_2O, H_2, O, O_3, NO, NO_2 and HNO_3. *Molina-Cuberos et al.* [2002] have used this model atmosphere to study the lower ionosphere of Mars. Later *Haider*

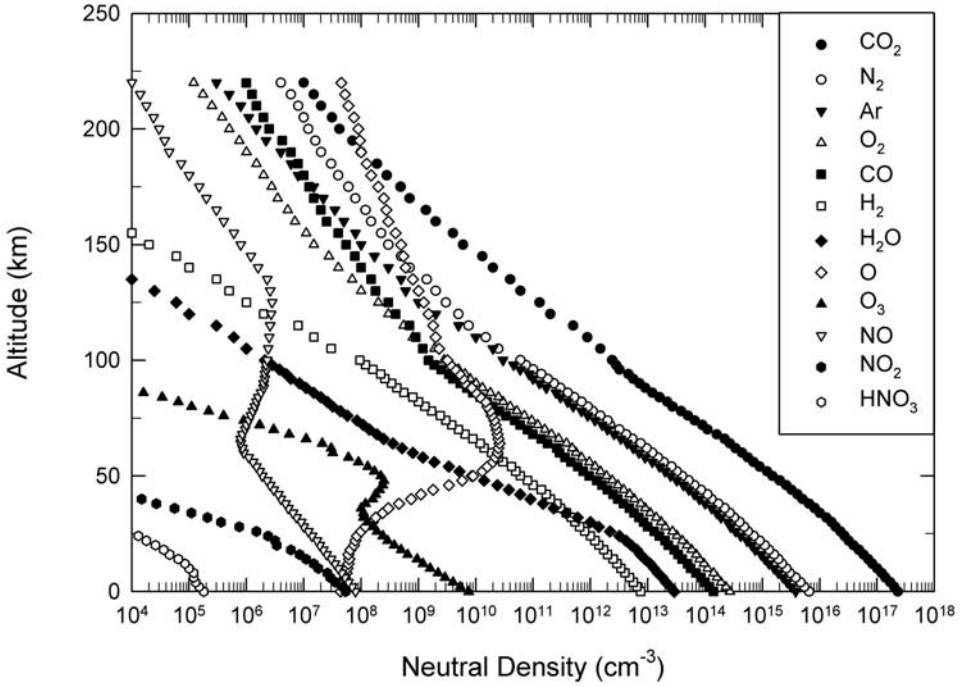

Figure 1. Neutral densities of CO_2, N_2, Ar, O_2, CO, H_2O, H_2, O, O_3, NO, NO_2, and HNO_3 in the daytime atmosphere above the surface of Mars.

et al. [2008] obtained model of the troposphere at high-latitude terminator region using the mixing ratios of these gases by multiplying it with the air density observed from MGS. In this paper we have constructed a model atmosphere of 12 gases CO_2, N_2, H_2, Ar, O_2, CO, H_2O, O_3, O, NO, NO_2 and HNO_3 from these references at different altitudes between 0 km and 220 km, which is plotted in Figure 1. Linear interpolation method was used wherever the data is not available in these height intervals. A maximum O_3 density is produced at an altitude of ~50 km owing to recombination of O and O_2 in three body reaction with CO_2. Below 40 km, O is mainly destroyed by H_2 and H_2O. Above this altitude, it combines to form O_2. Therefore, the density of O represents a broad peak at about ~60 km. NO_2 and HNO_3 contents are decreasing very rapidly with height in altitude region near the surface but they are important for nitrogenated chemistry. Using this model atmosphere, densities of 35 ions are calculated under steady state photochemical equilibrium condition. The electron density is calculated using charge neutrality condition. The chemical reactions and their rate coefficients are taken from *Molina-Cuberos et al.* [2002] and *Haider et al.* [2007, 2008]. The temperature is taken from *López-Valverde et al.* [1998] and *Bougher et al.* [1999]. The rate coefficient for most three body reactions are measured using N_2 or O_2 as third body. We follow the convention of *Molina-Cuberos et al.* [2002], where CO_2 is assumed to have the same efficiency as O_2 or N_2. The flux of incident galactic cosmic rays is taken from *Haider et al.* [2008].

[8] In our calculation the solar flux, branching ratios, photoabsorption, photoionization, elastic and inelastic cross sections are taken from other references [cf. *Torr and Torr*, 1979; *Tobiska et al.*, 2000; *Haider et al.*, 2002, 2006]. The solar flux, photodissociation and electron photodetachment reactions are observed at 1 AU. They are scaled by $1/R^2$ at Mars, where R is the heliocentric distance equal to 1.52 AU. The photoelectron spectrum is calculated owing to absorption of solar EUV and X-ray radiations of wavelengths range 9–102.5 nm and 1–9 nm, respectively. The production rates are calculated by using two dimensional yield spectrum and cosmic ray energy loss models. These models are described in section 4. The production rates have been used later in the continuity equation to calculate the ion and electron density.

4. Methods

4.1. Two-Dimensional Yield Spectrum Model

[9] The yield spectrum approach is presented in terms of two and three dimensions by using Monte Carlo technique [*Haider and Singhal*, 1983; *Singhal and Haider*, 1984]. We have used earlier three dimensional yield spectrum approach to calculate the ion production rates owing to precipitation of solar wind electron in the nighttime atmosphere of Mars [*Seth et al.*, 2002; *Haider et al.*, 2007]. These calculations were carried out in the presence of a vertical magnetic field of solar wind. In the present paper we have applied two dimensional yield spectrum model to calculate photoelectron impact ionization rates in the dayside ionosphere of Mars. This approach is used where the magnetic field of solar wind is horizontal in direction such as observed by MGS in the dayside ionosphere of Mars at high latitude [*Ness et al.*, 2000]. In this model the photoelectrons loose their energy at the same height where they are produced. Thus the vertical transport of photoelectrons is inhibited. The photoelectron impact ionization rates are calculated as given below:

$$J(h,\chi) = \int_{W_i}^{\infty} dE_o \int_{E}^{\infty} R_i(h,\chi,E) U^c(E,E_o) p_i(E) dE, \quad (1)$$

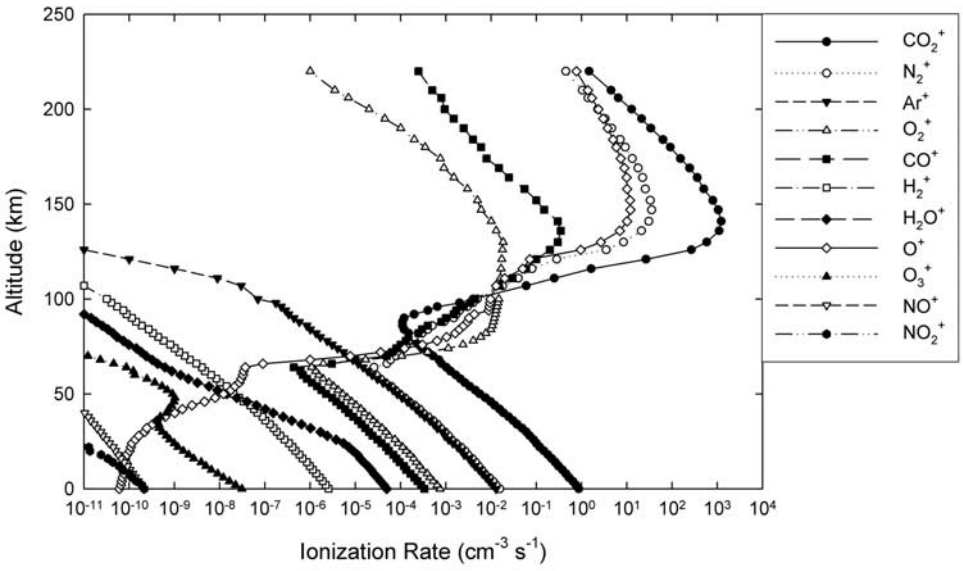

Figure 2. Model calculation of ion production rates of CO_2^+, N_2^+, Ar^+,O_2^+, CO^+, H_2O^+, H_2^+, O^+, O_3^+, NO^+, and NO_2^+ above the surface of Mars at solar zenith angle 77°.

where $J(h,\chi)$ is the photoelectron impact ionization rate at altitude h and solar zenith angle χ, the primary photoelectron spectrum $R_i(h,\chi,E)$ is calculated by *Seth et al.* [2006a, 2006b] at solar zenith angle 77 degree using generalized Chapman function as given by *Smith and Smith* [1972], the photoionization rate $R_i(h,\chi)$ is obtained from primary photoelectron spectrum $R_i(h,\chi,E)$ by integrating it over energy E, i represents ith gas, E_o is incident energy of monoenergetic electrons, which were introduced in a gas medium, E is the energy of secondary or tertiary electrons, which are calculated at that time when primary electrons ionize the atmospheric gases, and $U^c(E,E_o)$ is two dimensional composite yield spectrum at energy E_o and E. The composite yield spectrum approach is obtained by weighting the component of yield spectrum $U(E,E_o)$ as given below:

$$U^c(E,E_o) = \sum_i f_i U_i(E,E_o) \tag{2}$$

$$U_i(E,E_o) = C_0 + C_1 X + C_2 X^2 \tag{3}$$

$$X = \frac{(E_o/1000)^{0.585}}{E+1}. \tag{4}$$

In this equation C_0, C_1 and C_2 are adjustable parameters of different gases, which are given by *Singhal and Green* [1981]. The value f_i is the fractional composition and is given by

$$f_i = \frac{S_i n_i(h)}{\sum_j S_j n_j(h)}, \tag{5}$$

where S_i/S_j is the average value of $\sigma_{Ti}(E)/\sigma_{Tj}(E)$ between E_{min} = 2 eV to E_o, $\sigma_{T_i}(E)$ is the total (elastic and inelastic) cross sections, which are taken from *Porter and Jump* [1978] and *Jackman et al.* [1977] and $n_i(h)$ is the neutral density. Here $p_i(E)$ is the ionization probability which is calculated from the following equation:

$$p_i(E) = \frac{n_i(h)\sigma_i(E)}{\sum n_i(h)\sigma_{T_i}(E)}, \tag{6}$$

where $\sigma_i(E)$ is the ionization cross section.

4.2. Cosmic Ray Energy Loss Model

[10] The high-energy cosmic rays propagate through the atmosphere producing nucleonic cascades. The impact of primary cosmic rays, mainly protons and α particle with the atmospheric molecules produces protons, neutrons and pions. Fast secondary nucleons can gain enough energy to increase the production of particles by neutral collisions. Neutral pions quickly decay to gamma rays, and their contribution to the energy deposition is very important in the lower part of the atmosphere. At high-altitude level the maximum ion production rates are due to protons. Charged pions decay to muons, which do not decay before reaching the ground, and hence the muon energy is transferred to the surface. The ion production rates owing to absorption of galactic cosmic rays at solar zenith angle χ are given below:

$$q(h,\chi) = \frac{1}{Q}\int_E \int_\Omega (dE/dh)F(\chi,E,\Omega)d\Omega dE, \tag{7}$$

where Q = 35 eV is the energy required for the formation of an electron ion pair; (dE/dh) is the ionization loss of the gas, F is the total differential flux and Ω is the spatial angle. The formulae of the total differential flux of galactic cosmic rays and their attenuation loss in the Martian atmosphere have been derived in detail by *Haider et al.* [2008]. Therefore, they are not given in this paper. Since the cosmic

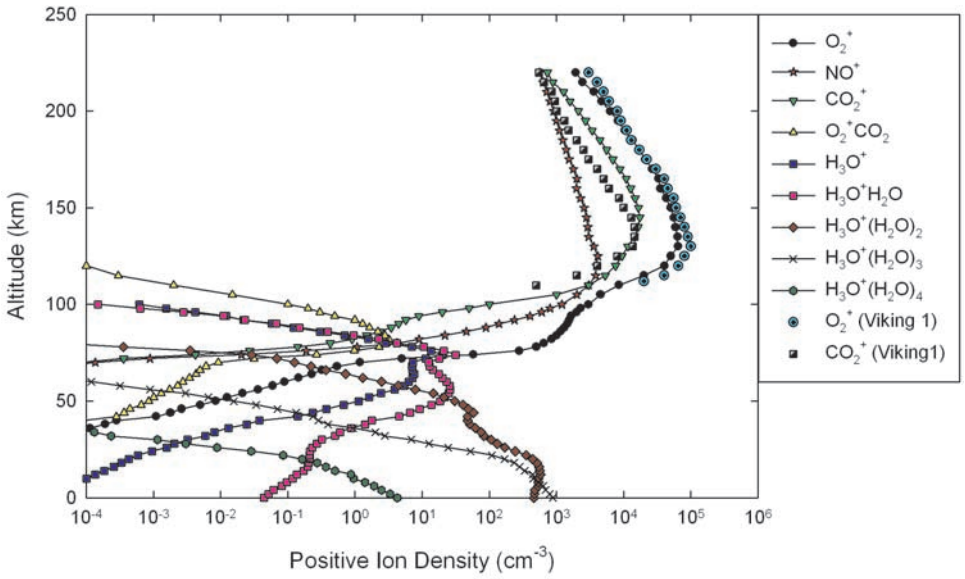

Figure 3. Altitude profiles of positive ion densities of O_2^+, NO^+, CO_2^+, $O_2^+CO_2$, H_3O^+, $H_3O^+H_2O$, $H_3O^+(H_2O)_2$, $H_3O^+(H_2O)_3$, and $H_3O^+(H_2O)_4$ owing to impact of solar EUV, X ray, and galactic cosmic rays with the atmosphere of Mars at solar zenith angle 77°. The measured profiles of Viking1 for CO_2^+ and O_2^+ are also plotted in this figure.

rays penetrate isotropically into the atmosphere, equation (7) reduces as follows:

$$q(h,\chi) = \frac{2\pi}{Q}\int (dE/dh)F(\chi,E)dE. \quad (8)$$

5. Results and Discussion

5.1. Production Rates and Densities of Positive and Negative Ions on Mars

[11] In Figure 2 we represent production rates of 11 ions, CO_2^+, N_2^+, Ar^+, O_2^+, H_2^+, CO^+, H_2O^+, O^+, O_3^+, NO^+ and NO_2^+ at solar zenith angle 77° owing to impact of solar EUV and X ray (photoionization + photoelectron) and galactic cosmic rays production with atmosphere of Mars (the production rate of HNO_3^+ has insignificant value, therefore, this is not plotted in Figure 2). As expected solar EUV and X rays are the major sources above 80 km, while ionization produced by galactic cosmic rays is dominant below this altitude. The total ion production rates are obtained by adding solar EUV, X ray and galactic cosmic ray ionizations. The maximum ionization rates of CO_2^+, N_2^+, O^+, CO^+ and O_2^+ are found to be $\sim 1.2 \times 10^3$ cm^{-3} s^{-1}, 3.6×10^1 cm^{-3} s^{-1}, 1.2×10^1 cm^{-3} s^{-1}, 3.5×10^{-1} cm^{-3} s^{-1} and 1.8×10^{-2} cm^{-3} s^{-1} at altitudes 141 km, 146 km, 147 km, 136 km and 130 km, respectively. The production rates of Ar^+, H_2^+, H_2O^+, O_3^+, NO^+ and NO_2^+ are significantly low above 80 km. These ions are mainly produced by ionization owing to galactic cosmic rays. The production rates shown in Figure 2 are used in the calculation of the densities of 35 ions (Ar^+, O_2^+, CO_2^+, $O_2^+CO_2$, NO^+, H_3O^+, $H_3O^+H_2O$, $H_3O^+(H_2O)_2$, $H_3O^+(H_2O)_3$, $H_3O^+(H_2O)_4$, H_3O^+HO, $CO_2^+CO_2$, CO^+, C^+, N_2^+, NO^+CO_2, N^+, $O_2^+(CO_2)_2$, $O_2^+H_2O$, $O_2^+(H_2O)_2$, O_4^+, O^+, $CO_3^-H_2O$, $CO_3^-(H_2O)_2$, CO_3^-, CO_4^-, NO_2^-, $NO_2^-H_2O$, $NO_2^-(H_2O)_2$, NO_3^-, $NO_3^-H_2O$, $NO_3^-(H_2O)_2$, O_2^-, O_3^-, and O^-).

[12] Of 35 ions the number densities of nine major positive ions, O_2^+, NO^+, CO_2^+, $O_2^+CO_2$, H_3O^+, $H_3O^+H_2O$, $H_3O^+(H_2O)_2$, $H_3O^+(H_2O)_3$, and $H_3O^+(H_2O)_4$ are shown in Figure 3. The measured profiles of Viking1 for CO_2^+ and O_2^+ are also represented in this figure. Unfortunately, there is no measurement of the concentration of cations and anions below 115 km. Above this height, the densities of CO_2^+, O^+ and O_2^+ are measured by retarding potential analyzer instrument onboard Viking 1 and 2 Landers [*Hanson et al.*, 1977]. This experiment did not observe NO^+, while O^+ was measured above ~180 km. Initially CO_2^+ is produced owing to impact of solar EUV, X ray and galactic cosmic rays with the daytime atmosphere of Mars. The other production mechanism of CO_2^+ is obtained from the loss of N_2^+, Ar^+ and CO^+ with CO_2.This ion is quickly removed by atomic oxygen leading to O_2^+ as a dominant ion. The ion NO^+ is formed owing to destruction of O_2^+ with NO. These ions are entirely destroyed by dissociative recombination process. The production of O^+ is quite abundant in the upper atmosphere. This ion is mostly destroyed by CO_2. This is a very fast reaction to permit the development of a significant layer of O_2^+ in the *F* region. The ions, O_2^+, NO^+, and CO_2^+ are dominant above 70 km. The peaks of O_2^+, CO_2^+ and NO^+ are located at altitudes ~130 km, 145 km and 125 km with the values $\sim 6.4 \times 10^4$ cm^{-3}, 1.7×10^4 cm^{-3} and 4.1×10^3 cm^{-3}, respectively. In this region the densities of O_2^+ and NO^+ are approximately related as $[O_2^+] \alpha [CO_2^+][O]/[N_e]$ and $[NO^+] \alpha [O_2^+][NO]/[N_e]$, respectively, where $[CO_2^+]$ and $[N_e]$ are the ion and electron densities, respectively. There has been found good agreement between calculated and measured densities of CO_2^+ and O_2^+. Below 70 km, nearly 100% $O_2^+CO_2$ is formed owing to three body

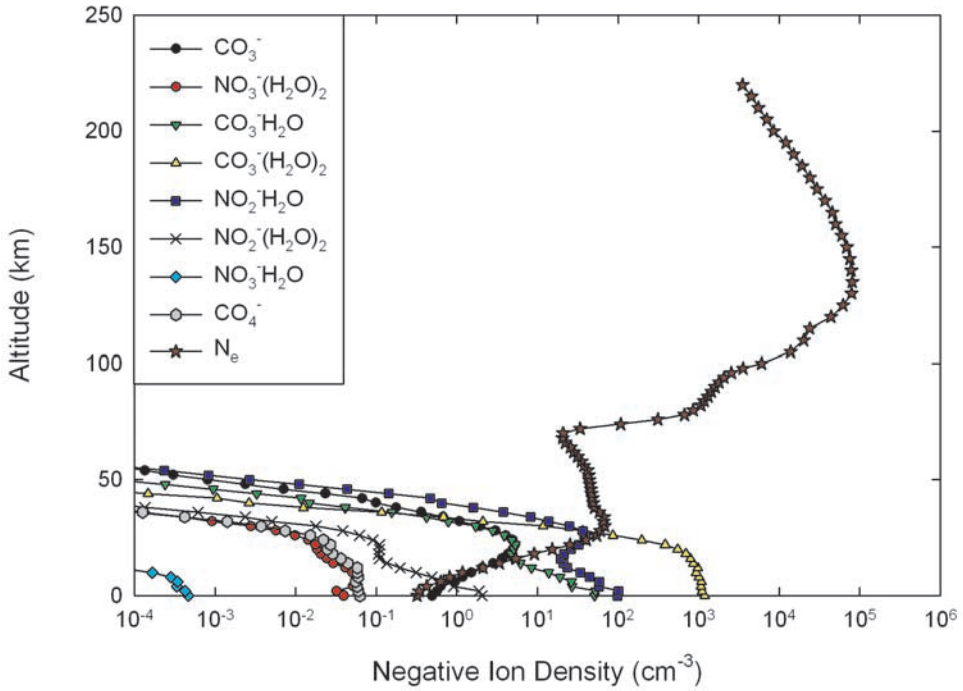

Figure 4. Altitude profiles of negative ion densities of electron, CO_3^-, $NO_3^-(H_2O)_2$, $CO_3^-H_2O$, $CO_3^-(H_2O)_2$, $NO_2^-H_2O$, $NO_2^-(H_2O)_2$, $NO_3^-H_2O$, and CO_4^- owing to impact of solar EUV, X ray, and galactic cosmic rays with the atmosphere of Mars at solar zenith angle 77°.

reaction, which is fully destroyed by water vapor in the formation of H_3O^+ (The production of NO^+CO_2 is significantly low from $O_2^+CO_2$). Once H_3O^+ has been produced water molecules are associated into it to form hydrated hydronium ions $H_3O^+(H_2O)_n$. We have considered the reactions of production and loss to form the hydronium ions up to four water molecules. The dissociative recombination of $H_3O^+(H_2O)_n$ are always smaller than any other loss processes at low-altitude region. These ions have been measured in Earth's ionosphere by sounding rockets carrying ion mass spectrometer [*Zbinden et al.*, 1975]. We have neither in situ measurements of low-altitude ion layers nor remote sensing measurements from the Martian surface.

[13] In Figure 4 the number densities of eight major negative ions CO_3^-, $NO_3^-(H_2O)_2$, $CO_3^-(H_2O)$, $CO_3^-(H_2O)_2$, $NO_2^-H_2O$, $NO_2^-(H_2O)_2$, $NO_3^-H_2O$, CO_4^- and electron are shown. Initially negative ions O^- and O_2^- are produced through electron capture by ozone and molecular oxygen, respectively. Later CO_3^- and CO_4^- are produced by three body reactions $O^- + CO_2 + M \rightarrow CO_3^- + M$ and $O_2^- + CO2 + M \rightarrow CO_4^- + M$, respectively. The ion CO_4^- is destroyed by atomic oxygen producing CO_3^- whose peak density occurs at altitude ~28 km with a value of ~8 cm^{-3}. The loss of CO_3^- with H_2O is a major source of $CO_3^-(H_2O)_n$, which are entirely destroyed by photodissociation above 40 km. Below this height these reactions are important for the production of nearly 100% $CO_3^-(H_2O)_2$ ion. The ion CO_3^- is also destroyed by NO and NO_2 forming NO_2^- and NO_3^-, respectively. Later NO_2^- and NO_3^- are associated with water vapor through three body reactions producing $NO_2^-(H_2O)_n$ and $NO_3^-(H_2O)_n$, respectively, which are dissociated with neutral collision. The ion $CO_3^-H_2O$ is partially destroyed by NO to produce second major ion $NO_2^-H_2O$.

5.2. Comparison of Electron Density Distribution on Mars and Earth

[14] Before a more detailed comparison between the ionospheres of Mars and Earth is presented, it would be useful to recall the more salient characteristics of these planets and their atmospheres that affect the electron density distribution. (1) The flux of the solar ionizing radiation (EUV), being inversely proportional to the square of the distance from the sun, is half or less as intense on Mars as it is on Earth. (2) In the region where most of the energies of EUV, X rays, and galactic cosmic rays are absorbed, the atmosphere consists largely of CO_2 on Mars and of O, O_2, and N_2 on Earth. (3) The dayside ionosphere of Mars consists of a thin *F* layer with a peak electron concentration near 10^5 cm^{-3}, while the ionosphere of Earth extends over several hundred kilometers with a peak concentration ~4 times larger. (4) The propagation of cosmic rays is affected by the solar wind in the interplanetary medium and in the vicinity of the magnetic planets by their intrinsic fields. The magnetic field on Mars is not high enough as of Earth to affect the cosmic raypath. The effect of the solar wind interaction with cosmic rays can be considered similar at Earth and Mars and therefore the same modulation of the cosmic rays owing to solar wind for solar minimum activity at Earth is used for Mars. Most of these characteristics are subject to substantial variations with solar activity, planetary season, and position within the planetary atmosphere, which must be also taken into consideration in a detailed comparison of the ionospheres of these planets. Such a comparison is beyond the scope of the present study, but we will compare our model calculation and radio occultation observations of Mars with a specific electron density pro-

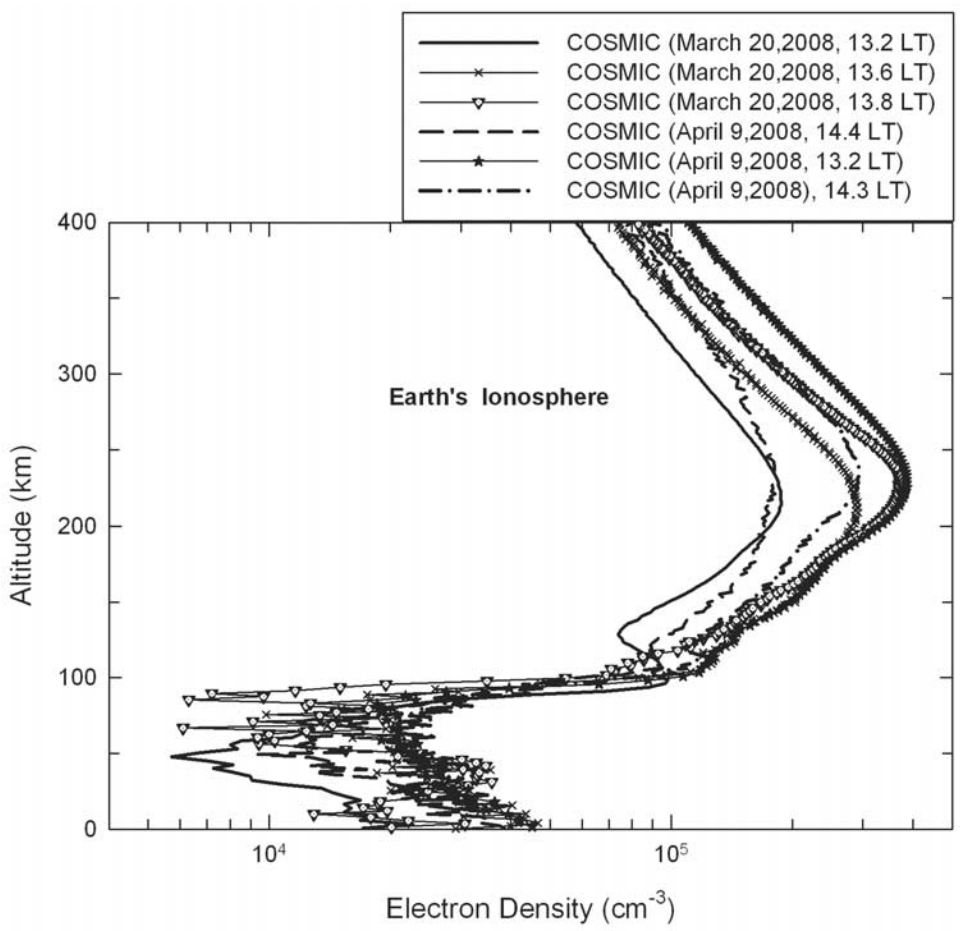

Figure 5. Six sample profiles of electron density representing *D*, *E*, and *F* layers as observed in Earth's ionosphere by radio occultation experiment on board COSMIC satellites at different locations at nearly the same local time in the afternoon.

file of Earth's ionosphere pertaining to nearly similar physical conditions.

[15] Figures 5 and 6 show the sample profiles of electron density observed at nearly the same time, location and solar conditions in the ionospheres of Earth and Mars, respectively. We have selected six profiles in Earth's ionosphere from COSMIC measurements carried out on 20 March and 9 April 2008 at coordinates (72.7°N 153.4°W), (51.8°N 49.5°W), (49.8°N 144.5°W) and (67.3°N 146°W), (54°N 126.3°W), (58.4°N 93.6°W), respectively. These observations are carried out in the afternoon at nearly the same local time (13.2, 13.6, 13.8, 14.4, 13.2 and 14.3) during low solar activity period ($F_{10.7} = 68$). In these measurements *F* peak is always clearly present while *D* and *E* peaks sometimes appear as a shoulder and sometimes as a separate peak. The nonzero values of electron density below ~50 km altitude (where the density in theory should be almost zero) give an indication of the uncertainty of the profiles retrievals. This uncertainty is caused by the horizontal gradients of density not having been taken into account in the inversion of the occultation data [*Anthes et al.*, 2008]. These profiles of electron density are nearly identical. Their peak densities and peak heights are changing with different locations of the observations. The Martian ionospheric profiles of Figure 6 were obtained from observations by MGS, Mars 4 and Mars 5. Six profiles of electron density have been selected from MGS observations carried out on 20 March and 9 April 2005 at coordinates (74.4°N 106.5°W), (74.3°N 49.2°W), (74.2°N 209°W) and (70°N 156°W), (70°N 127°W), (70°N 99°W), respectively. (The data are not available in 2008 because MGS failed to work since 2006.) These observations were also performed in the afternoon (solar zenith angle 77°) at nearly same local time (12.95, 12.96, 12.97, 13.75, 13.76 and 13.74) with low solar activity period ($F_{10.7} = 39$). These measurements show two ionization peaks at altitude ~125–145 km and 100–115 km similar to that observed as *F* and *E* peaks in Earth's ionosphere [*Bougher et al.*, 2001; *Haider et al.*, 2006]. The first peak is always observed to be $\sim 8.6 \times 10^4$ cm^{-3} in the dayside ionosphere of Mars. The second (lower) peak sometimes appears as a shoulder and sometimes as a separate peak with value $\sim 2-4 \times 10^4$ cm^{-3}. The third layer is clearly evident in one profile of MGS observations at altitude ~80 to 100 km where electron density peaked at 8×10^3 cm^{-3} which corresponds to an increase by 2 to 8 times of one standard deviation of the electron density fluctuations. This layer has also been observed by Mars Express [*Patzold et al.*, 2005]. Its origin could be associated to ablation process in which metallic ions were formed by charge exchange with atmospheric ions.

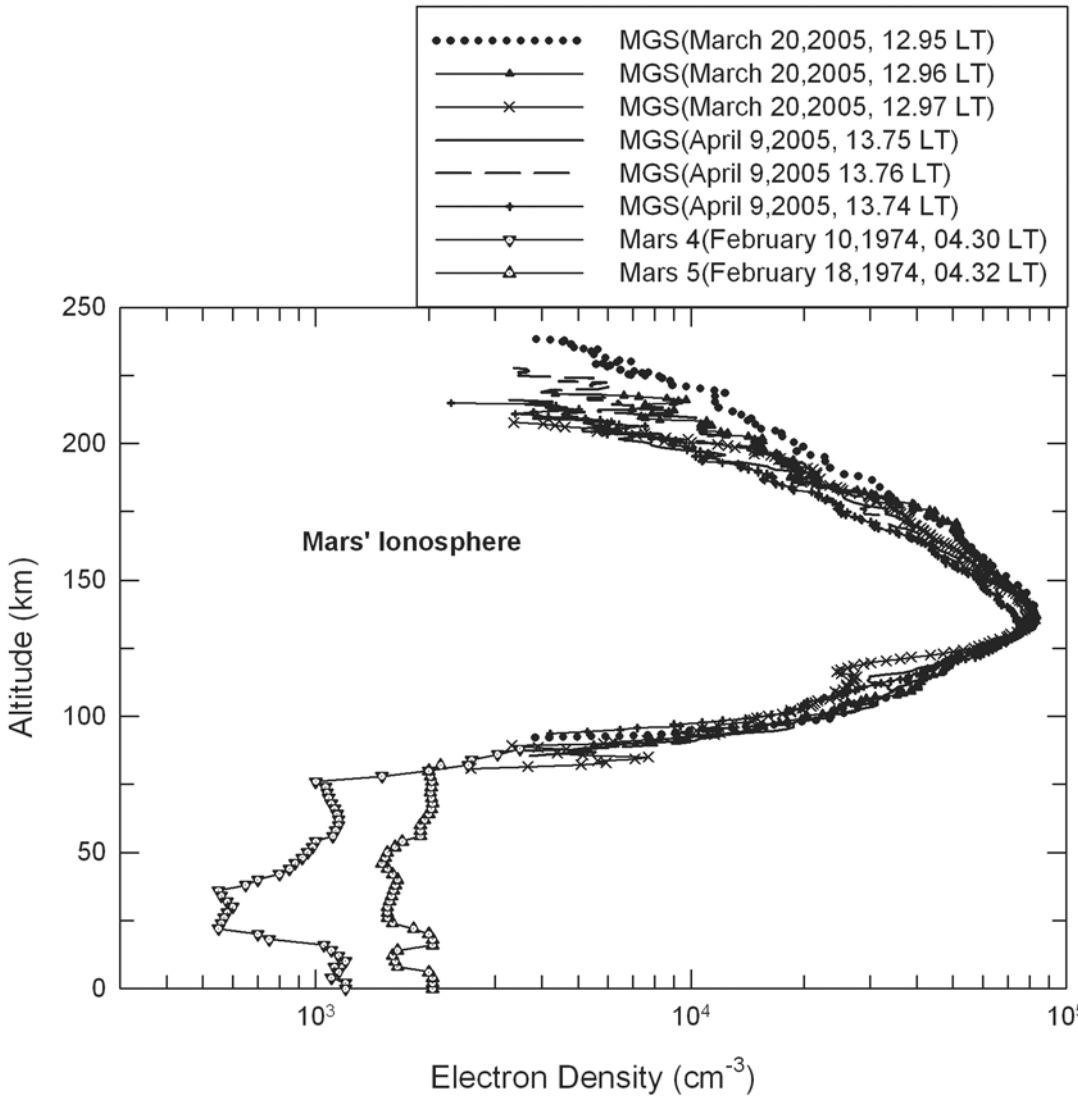

Figure 6. Six sample profiles of electron density representing *E* and *F* layers in the Martian ionosphere as observed by radio occultation experiment on board MGS at nearly the same local time in the afternoon. Density profiles representing *D* layer is shown by radio occultation measurements on board Mars 4 and Mars 5 at evening.

[16] The complete profile of electron density representing *D*, *E*, and *F* layers is not observed in the dayside ionosphere of Mars. MGS did not measure electron density below ~80 km [*Hinson et al.*, 2001], where Mars 4 and Mars 5 have observed electron density on 10 and 18 February 1974 under low solar activity period at local time 0430 with solar zenith angle 106° [*Savich and Samovol*, 1976]. These measurements showed a broad peak between altitude 35 km and 70 km as observed in the *D* region of Earth's ionosphere. In Figure 6 we have plotted electron density between 0 km and 80 km from these measurements to obtain a complete electron density profile above the surface of Mars. It may be noted that the electron density depends on the solar zenith angle χ by $N_e = N_0 (\cos \chi)^{\alpha}$, where α is between 0.2 and 0.7, N_0 is electron density for zero solar zenith angle. In the *D* region ionosphere of Earth, electron density is decreased by factor of ~2 between solar zenith angle 77° and 106° [*Friedrich and Torkar*, 1992]. However, dependence of electron density on solar zenith angle is insignificant in the dayside upper ionosphere of Mars at terminator region. *Bougher et al.* [2004] did not find a clear trend of electron density with solar zenith angle in the 448 profiles of MGS data set at *F* region (125–145 km) between solar zenith angles 75° and 87°. *Haider et al.* [2006] using 32 electron density profiles of MGS found that *E* region (100–112 km) electron densities are independent on solar zenith angles between ~77° and 82°. Recently *Mahajan et al.* [2007] have analyzed 807 electron density profiles of MGS. They have also reported that electron densities of *E* and *F* regions do not depend on solar zenith angles between 75° and 87°. However, it is changed by a factor of ~1.1 in the topside ionosphere (160–170 km) at same solar zenith angle interval. MGS did not measure electron density in the upper ionosphere at solar zenith angle >87°. Therefore, we do not know from MGS observations how much electron density is decreased at the terminator upper ionosphere of Mars after sunset. In the *D*

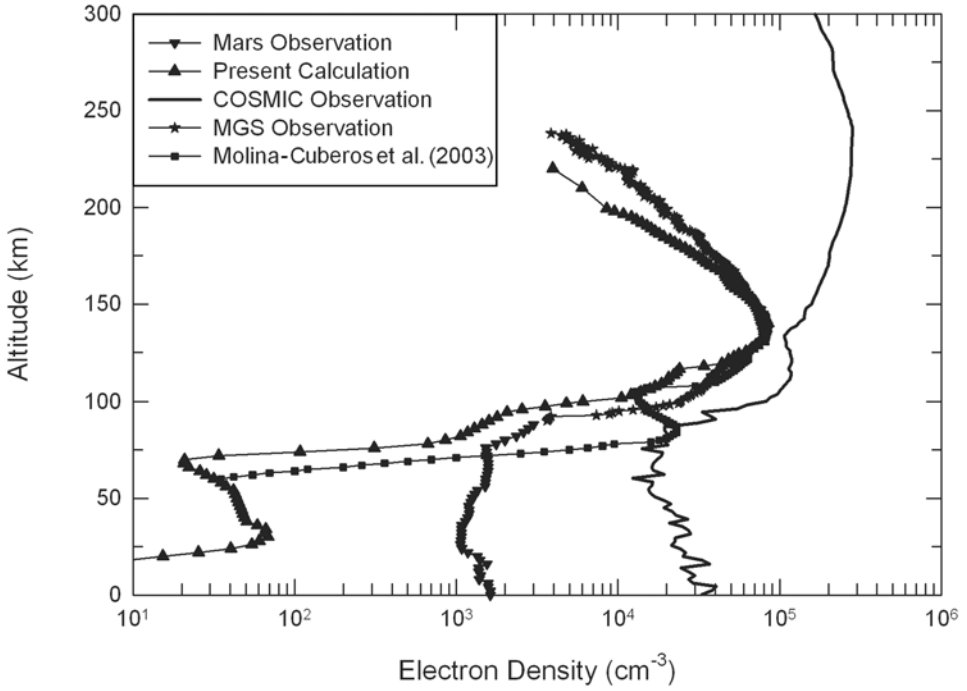

Figure 7. Calculated and measured electron density profiles representing *D*, *E*, and *F* layers in the ionospheres of Mars and Earth. Solid line is the mean electron density of Figure 5 as observed in Earth's ionosphere at afternoon by radio occultation experiment onboard COSMIC satellites. Line with star is the mean electron density of Figure 6 as observed in the Martian ionosphere at solar zenith angle 77° by radio occultation experiment on board MGS. Line with downward triangle is the mean electron density of Figure 6 (below 80 km) as observed in the Martian ionosphere at solar zenith angle 106° by radio occultation experiment onboard Mars 4 and Mars 5. Present calculation is represented by line with filled upward triangle in the Martian ionosphere at solar zenith angle 77°. Calculation of *Molina-Cuberos et al.* [2003] is represented by the solid line with squares.

region our previous calculation suggests that cosmic ray absorption in the Martian atmosphere is nearly the same between solar zenith angles 77° and 106° because the atmospheric thickness along the slant paths does not change significantly at these angles [*Haider et al.*, 2007]. In the dayside ionosphere of Mars we have neither in situ measurements of low-altitude ionosphere nor remote sensing measurements from Mars surface. The direct measurement of *D* region ionosphere can be performed in future by Langmuir probe experiment onboard Mars Lander. This experiment has been used in rockets and balloons to measure the lower ionosphere of Earth. In the absence of *D* region electron density measurement on Mars at solar zenith angle 77°, we have used Mars 4/5 observations available at solar zenith angle 106°. Future measurement will confirm the solar zenith angle dependence of *D* region ionosphere at Mars.

[17] In Figure 7 the present calculation is compared with the mean electron density profiles obtained from COSMIC observation shown in Figure 5 and from MGS and Mars 4/5 observations shown in Figure 6 for the ionospheres of Earth and Mars, respectively. In our calculation the first, second and third peaks are produced at altitudes ~125–145 km, 100–112 km and 25–35 km owing to absorption of solar EUV (90–1026 Å), X ray (10–90 Å) and galactic cosmic ray (1–1000 GeV) radiations, respectively, in the Martian ionosphere. These peaks are represented as *F*, *E*, and *D* layers similar to that observed in Earth's ionosphere. *F* and *E* peaks are mainly controlled by photoionization and photoelectron impact ionization processes. These peaks are not very much distinct owing to use of combined solar radiation at wavelength region 1–102.6 nm. Our previous calculation represented *F* and *E* peaks separately at altitude ~140 km and ~108 km with values of $\sim 8.5 \times 10^4$ cm^{-3} and $\sim 2.0 \times 10^4$ cm^{-3}, respectively [*Haider et al.*, 2002]. The calculated plasma density in the *D* layer is smaller by factor of ~15 compared to that measured by Mars. However, its position beyond ~50 km is comparable with the observation. This difference between theory and experiment could be attributed to possible errors of the measurements. The presence of plasma in the lower ionosphere of Mars is derived on the basis of the formal inversion of the set of observations in symmetrical approximation. During the occultation measurements, the possible displacement of electron density owing to this error was estimated to be $\approx \pm 500$ cm^{-3} [*Savich and Samovol*, 1976]. The other reason for the error perhaps is that the ion and electron densities could not be separated out by Mars 4/5 radio occultation measurements. If it is true, the calculated total (ion + electron) density can be brought into close agreement with the measurement.

[18] In comparing our *D* region electron density with the theoretical calculations performed by *Whitten et al.* [1971] and *Molina-Cuberos et al.* [2002], we find a good agreement at all altitudes with the model calculation of *Molina-Cuberos et al.* [2002], who used the same model atmosphere as we used. In both model calculations *D* peak is located at

Table 1. *D*, *E*, and *F* Layers in the Dayside Ionospheres of Mars and Earth

	Peak Densities			Peak Heights		
	Mars Model (cm^{-3})	Mars Observation (cm^{-3})	Earth Observation (cm^{-3})	Mars Model (km)	Mars Observation (km)	Earth Observation (km)
F peak	8.4×10^4	8.6×10^4	3.0×10^5	~125–145	~125–145	~200–250
E peak	2.4×10^4	3.5×10^4	1.0×10^5	~100–112	~100–115	~90–120
D peak	7.0×10^1	$\sim 1.5 \times 10^3$	$\sim 1.8 \times 10^4$	~25–35	~40–65	~65–75

altitude ~25–35 km with a value of ~70–100 cm^{-3}. Our *D* layer is less by a factor of ~5 as compared to that calculated by *Whitten et al.* [1971] as ~400–500 cm^{-3} at altitude ~25–35 km. This difference is due to several reasons: (1) *Whitten et al.* [1971] did not include nitrogenated chemistry in their model. The inclusion of nitrogenated molecules NO, NO_2 and HNO_3 is very important in the chemistry of negative ions. These reactions reduce electron density in the *D* region ionosphere of Mars. (2) They have used only 29 chemical reactions versus 133 used by us with better understanding of the chemistry of the terrestrial *D* region that can be directly applied to Mars. (3) Finally, the improvement of neutral modeling at Mars together with the data obtained from Viking 1/2 and Mars pathfinder has provided a better knowledge of neutral composition and structure compared to what was used previously by *Whitten et al.* [1971]. The density profiles of atomic oxygen and ozone, which have high influence on the chemistry of negative ions are now more realistic. We have used updated model atmosphere of 12 gases as reported by *Molina-Cuberos et al.* [2002]. In Figure 7 the present calculation is also compared with the model calculation of *Molina-Cuberos et al.* [2003] that was based on meteoric ablation in the daytime ionosphere of Mars. The chemistry of meteoric ions (Ca^+, Mg^+ and Fe^+) is not used in the present model. Therefore, the metal ion layer is not seen in our calculated electron density profile. *Molina-Cuberos et al.* [2003] have reported the existence of metal ions (Fe^+ and Mg^+) layer at altitude ~85 km. In presence of meteoric ions the electron concentration is increased by about an order of magnitude between altitude 60 km and 90 km.

[19] *D* layer in the dayside ionosphere of Earth is observed at altitude ~65–75 km mainly owing to solar Lyman α radiation ionizing minor constituent NO. Galactic cosmic rays, which affect the whole atmosphere down to the ground, become a major ionization source in the lower *D* region [cf. *Schunk and Nagy*, 2000]. X rays do not contribute significantly to *D* region ionosphere of Earth at sunspot minimum. At night the *D* layer begins to disappear because the primary source of ionization is no longer present and the cosmic rays produce a residual amount of ionization. The ionization owing to solar Lyman α is not studied in the lower ionosphere of Mars. This source will be almost ineffective because the density of NO is lower by ~2–3 orders of magnitude in the Martian mesosphere as compared to that observed in the mesosphere of Earth [cf. *Aikin*, 1968; *Hargreaves*, 1992]. The cosmic ray ionization has been found to be an important process for the formation of *D* layers in daytime and nighttime lower ionosphere of Mars [*Whitten et al.*, 1971; *Molina-Cuberos et al.*, 2002; *Haider et al.*, 2007]. The column densities in the atmospheres of Mars and Earth are nearly $\sim 2.3 \times 10^{27}$ m^{-2} and $\sim 2.2 \times 10^{29}$ m^{-2}, respectively. Therefore, cosmic rays penetrate deeper into the Martian atmosphere and form *D* layer at lower altitudes than that observed in Earth's ionosphere. The electron density in the *D* region of Earth's ionosphere is larger than that measured in the Mars's *D* region by an order of magnitude. The reason for this difference lies in the fact that the physical processes of *D* region ionospheres of Mars and Earth are quite different. *E* and *F* peaks in Earth's ionosphere are observed at altitude ~90–120 km and ~200–250 km with values $\sim 1.0 \times 10^5$ cm^{-3} and $\sim 3.0 \times 10^5$ cm^{-3}, respectively, that are larger by factor of ~3–4 and 3.5, respectively, than the corresponding values in the Mars' ionosphere. *F* peak height in Earth's ionosphere is higher by factor of 1.8 than in the Mars' ionosphere. However, the location of *E* region remains same in the ionospheres of Earth and Mars. Such relative characteristics are determined by several factors: (1) The mean neutral-scale height near EUV absorption peak is 2–3 times smaller for Mars than for Earth, the smaller gravitational acceleration of Mars being offset by the lower exospheric temperature and the larger mean molecular weight. (2) The upper ionospheres of Mars and Earth have different optical depths. Below 160 km the optical depth of Mars changes by 2 orders of magnitude in an interval of 40 km, while the optical depth of Earth below 300 km changes by same amount in an altitude interval nearly 4 times as large [cf. *Bauer*, 1973]. This implies that solar EUV energy is deposited within much smaller altitude range in the upper atmosphere of Mars as compared to the corresponding altitude range in the upper atmosphere of Earth. (3) Finally, the density of Earth's atmosphere is larger than that of Mars by a factor of ~1.2–1.5. This will result in larger ion production and hence increased electron density in the upper ionosphere of Earth. The calculated and measured peak densities and peak heights for the daytime ionospheres of Earth and Mars are given in Table 1.

6. Conclusions

[20] Using the solar EUV, X ray and galactic cosmic ray radiations, the altitude profiles of ion production rates and densities of positive ions, negative ions and electrons are calculated at solar zenith angle 77° above the surface of Mars. In this paper we have not used proton impact ionization source as introduced by *Kallio and Janhunen* [2001] because the dayside ionosphere caused by this process is smaller by an order of magnitude than that produced by solar EUV radiation [*Haider et al.*, 2002]. Our calculations are made at high latitude under photochemical steady state condition using yield spectrum and cosmic ray energy loss models. The full ion-neutral schemes of 133 chemical reactions have been employed in the model. The chemical chains employed are long and comprehensive. The chemistry of Ca^+, Mg^+, Si^+ and Fe^+ are not included in the

present chemical model. The calculated electron density is compared with the radio occultation measurements made by MGS and Mars 4/5 in the ionosphere of Mars and by COSMIC satellites in the ionosphere of Earth. The present calculation is also compared with the calculations of *Molina-Cuberos et al.* [2003] on the basis of meteoric ablation in the lower ionosphere of Mars. In presence of meteoric ions the electron density is increased by about an order of magnitude between altitude 60 km and 90 km. Our calculated results suggest that the daytime ionosphere of Mars can be divided into *D*, *E*, and *F* layers. *D* region is formed at altitude ~25–35 km owing to precipitation of galactic cosmic rays. *E* and *F* regions represent maximum ionization at ~100–112 km and ~125–145 km owing to photoionization + photoelectron impact ionization processes caused by X rays and solar EUV radiations, respectively. The calculated *E* and *F* peaks are in good agreement with the radio occultation measurements at Mars. The estimated plasma density in the *D* layer of Mars is smaller by one and two orders of magnitude than those observed in the ionospheres of Mars and Earth, respectively. The height of the *F* layer peak in Earth's ionosphere is higher by factor of 1.8 than that of Mars' ionosphere owing to their different heights of maximum optical depth. The locations of *E* region are nearly same in the ionospheres of both planets. The values of *E* and *F* peak densities are larger in Earth's ionosphere than in Mars' ionosphere by factors of ~3–4 and 3.5, respectively.

[21] **Acknowledgments.** Authors are thankful to Dave Hinson and G. L. Tyler, Stanford University Stanford, California, USA, for providing us MGS radio science data of electron density profiles through the Web site http://nova.stanford.edu/projects/mgs/dmwr.html. Development of the COSMIC Data Analysis Archival Center is primarily supported by National Science Foundation and the National Oceanic and Atmospheric Administration. COSMIC data are provided by Taiwan's National Space Organization and University Corporation for Atmospheric Research. S. A. Haider also thanks FAPESP for the support through a visiting scientist fellowship by the process 2007/06736–8 to work at INPE, Brazil.

[22] Amitava Bhattacharjee thanks the reviewers for their assistance in evaluating this paper.

References

Acuna, M. H., et al. (1998), Magnetic field and plasma observations at Mars: Initial results of the Mars Global Surveyor Mission, *Science*, *279*, 1676–1680, doi:10.1126/science.279.5357.1676.

Aikin, A. C. (1968), The lower ionosphere of Mars, *Icarus*, *9*, 487–497, doi:10.1016/0019-1035(68)90042-0.

Anthes, R. A., et al. (2008), The COSMIC/FORMOSAT-3 mission: Early results, *Bull. Am. Meteorol. Soc.*, *89*(3), 313–333, doi:10.1175/BAMS-89-3-313.

Banks, P. M., and G. Kockarts (1973), *Aeronomy*, Elsevier, New York.

Barth, C. A., and C. W. Hord (1971), Mariner ultraviolet spectrometer: Topography and polar cap, *Science*, *173*, 197–201, doi:10.1126/science.173.3993.197.

Bauer, S. J. (1973), *Physics of Planetary Ionospheres*, Springer, New York.

Biemann, K., T. Owen, D. R. Rushneck, A. L. Lafleur, and D. W. Howarth (1976), The atmosphere of Mars near the surface: Isotope ratios and upper limits on noble gases, *Science*, *194*, 76–78, doi:10.1126/science.194.4260.76.

Bougher, S. W., S. Engel, R. G. Roble, and B. Foster (1999), Comparative terrestrial planet thermosphere: 2. Solar cycle variation of global structure and winds at equinox, *J. Geophys. Res.*, *104*, 16,591–16,611, doi:10.1029/1998JE001019.

Bougher, S. W., S. Engel, D. P. Hinson, and J. M. Forbes (2001), Mars Global Surveyor radio science electron density profiles: Neutral atmosphere implications, *Geophys. Res. Lett.*, *28*, 3091–3094, doi:10.1029/2001GL012884.

Bougher, S. W., S. Engel, D. P. Hinson, and J. R. Murphy (2004), MGS radio science electron density profiles: Interannual variability and implications for the Martian neutral atmosphere, *J. Geophys. Res.*, *109*, E03010, doi:10.1029/2003JE002154.

Brasseur, G. P., and S. Solomon (2005), *Aeronomy of the Middle Atmosphere: Chemistry and Physics of the Stratosphere and Mesosphere*, Springer, New York.

Duru, F., D. A. Gurnett, D. D. Morgan, R. Modolo, A. F. Nagy, and D. Najib (2008), Electron densities in the upper ionosphere of Mars from the excitation of electron plasma oscillations, *J. Geophys. Res.*, *113*, A07302, doi:10.1029/2008JA013073.

Fjeldbo, G., A. Kliore, and B. Seidel (1970), The Mariner 1969 occultation measurement of the upper atmosphere of Mars, *Radio Sci.*, *5*, 381–386, doi:10.1029/RS005i002p00381.

Fjeldbo, G., et al. (1977), Viking radio occultation measurements of Martian atmosphere and topography: Primary mission covering age, *J. Geophys. Res.*, *82*, 4317–4324, doi:10.1029/JS082i028p04317.

Fox, J. L. (2005), Aeronomy, in *Handbook of Atomic and Optical Physics*, edited by G. F. Drake, pp. 1259–1290, Springer, New York.

Friedrich, M., and K. M. Torkar (1992), An empirical model of the nonauroral *D* region, *Radio Sci.*, *27*, 945–953, doi:10.1029/92RS01929.

Gurnett, D. A., et al. (2005), Radar soundings of the ionosphere of Mars, *Science*, *310*, 1929–1933, doi:10.1126/science.1121868.

Haider, S. A., and R. P. Singhal (1983), Analytical yield spectrum approach to electron energy degradation in Earth's atmosphere, *J. Geophys. Res.*, *88*, 7185–7189, doi:10.1029/JA088iA09p07185.

Haider, S. A., S. P. Seth, E. Kallio, and K. I. Oyama (2002), Solar EUV and electron- Proton-hydrogen atom produced ionosphere on Mars: Comparative studies of particle fluxes and ion production rates due to different processes, *Icarus*, *159*, 18–30, doi:10.1006/icar.2002.6919.

Haider, S. A., S. P. Seth, V. R. Choksi, and K. I. Oyama (2006), Model of photoelectron impact ionization within the high latitude ionosphere at Mars: Comparison of calculated and measured electron density, *Icarus*, *185*, 102–112, doi:10.1016/j.icarus.2006.07.010.

Haider, S. A., V. Singh, V. R. Choksi, W. C. Maguire, and M. I. Verigin (2007), Calculated densities of $H_3O^+(H_2O)_n$, $NO_2^-(H_2O)_n$, $CO_3^-(H_2O)_n$ and electron in the nighttime ionosphere of Mars: Impact of solar wind electron and galactic cosmic rays, *J. Geophys. Res.*, *112*, A12309, doi:10.1029/2007JA012530.

Haider, S. A., V. Sheel, V. Singh, W. C. Maguire, and G. J. Molina-Cuberos (2008), Model calculation of production rates, ion and electron densities in the evening troposphere of Mars at latitudes 67°N and 62°S: Seasonal variability, *J. Geophys. Res.*, *113*, A08320, doi:10.1029/2007JA012980.

Hanson, W. B., S. Sanatani, and D. R. Zuccaro (1977), The Martian ionosphere as observed by the Viking retarding potential analyzer, *J. Geophys. Res.*, *82*, 4351–4363, doi:10.1029/JS082i028p04351.

Hargreaves, J. K. (1992), *The Solar Terrestrial Environment: An Introduction to Geospace—The Science of the Terrestrial Upper Atmosphere, Ionosphere and Magnetosphere*, Cambridge Univ. Press, New York.

Hinson, D. P., G. L. Tyler, J. L. Hollingsworth, and R. J. Wilson (2001), Radio occultation measurements of forced atmospheric waves on Mars, *J. Geophys. Res.*, *106*, 1463–1480, doi:10.1029/2000JE001291.

Jackman, C. H., R. H. Garvey, and A. E. S. Green (1977), Electron impact on atmospheric gases: 1. Updated cross sections, *J. Geophys. Res.*, *82*, 5081–5090, doi:10.1029/JA082i032p05081.

Kallio, E., and P. Janhunen (2001), Atmospheric effects of proton precipitation in the Martian atmosphere and its connection to the Mars-solar wind interaction, *J. Geophys. Res.*, *106*, 5617–5634, doi:10.1029/2000JA000239.

Kelley, M. C. (1989), *The Earth's Ionosphere: Plasma Physics and Electrodynamics*, Elsevier, New York.

Kliore, A. J., et al. (1972), The atmosphere of Mars from Mariner 9 radio occultation measurements, *Icarus*, *17*, 484–493, doi:10.1016/0019-1035(72)90014-0.

López-Valverde, M. A., D. P. Edwards, M. López-Puertas, and C. Roldán (1998), Nonlocal thermodynamic equilibrium in general circulation models of the Martian atmosphere: 1. Effects of the local thermodynamic equilibrium approximation on thermal cooling and solar heating, *J. Geophys. Res.*, *103*, 16,799–16,811, doi:10.1029/98JE01601.

Ma, Y.-J., and A. F. Nagy (2007), Ion escape fluxes from Mars, *Geophys. Res. Lett.*, *34*, L08201, doi:10.1029/2006GL029208.

Ma, Y.-J., A. F. Nagy, I. V. Sokolov, and K. C. Hansen (2004), Three-dimensional, multispecies, high spatial resolution MHD studies of the solar wind interaction with Mars, *J. Geophys. Res.*, *109*, A07211, doi:10.1029/2003JA010367.

Mahajan, K. K., S. Singh, A. Kumar, S. Raghuvanshi, and S. A. Haider (2007), Mars Global Surveyor radio science electron density profiles: Some anomalous features in the Martian ionosphere, *J. Geophys. Res.*, *112*, E10006, doi:10.1029/2006JE002876.

Molina-Cuberos, G. J., H. Lichtenegger, K. Schwingenschuh, J. J. López-Moreno, and R. Rodrigo (2002), Ion-neutral chemistry model of the lower

ionosphere of Mars, *J. Geophys. Res.*, *107*(E5), 5027, doi:10.1029/2000JE001447.

Molina-Cuberos, G. J., O. Witasse, J. Lebereton, R. Rodrigo, and J. Lopez-Moreno (2003), Meteoric ions in the atmosphere of Mars, *Planet. Space Sci.*, *51*, 239–249, doi:10.1016/S0032-0633(02)00197-6.

Nair, H., M. Allen, A. D. Anbar, Y. L. Yung, and R. T. Clancy (1994), A photochemical model of the Martian atmosphere, *Icarus*, *111*, 124–150, doi:10.1006/icar.1994.1137.

Ness, N. F., M. H. Acuna, J. E. P. Connerney, A. J. Kliore, T. K. Breus, A. M. Krymskii, P. Cloutier, and S. J. Bauer (2000), Effects of magnetic anomalies discovered at Mars on the structure of the Martian ionosphere and solar wind interaction as follows from radio occultation experiments, *J. Geophys. Res.*, *105*, 15,991–16,004, doi:10.1029/1999JA000212.

Nier, A. O., and M. B. McElroy (1977), Composition and structure of Mars's upper atmosphere: Results from the neutral mass spectrometers on Viking 1 and 2, *J. Geophys. Res.*, *82*, 4341–4350, doi:10.1029/JS082i028p04341.

Nier, A. O., W. B. Hanson, A. Seif, M. B. McElroy, N. W. Spencer, R. J. Duckett, T. C. D. Knight, and W. S. Cook (1976), Composition and structure of the Martian atmosphere: Preliminary results from Viking 1, *Science*, *193*, 786–788, doi:10.1126/science.193.4255.786.

Owen, T., K. Biemann, D. R. Rushneck, J. E. Biller, D. W. Homarth, and A. L. Lafleur (1977), The composition of the atmosphere at the surface of Mars, *J. Geophys. Res.*, *82*, 4635–4644, doi:10.1029/JS082i028p04635.

Patzold, M., S. Tellmann, B. Hausler, D. Hinson, R. Schaa, and G. L. Tyler (2005), A sporadic third layer in the ionosphere of Mars, *Science*, *310*, 837–839, doi:10.1126/science.1117755.

Porter, H. S., and F. W. Jump Jr. (1978), Analytical total and angular elastic electron impact cross section for planetary atmospheres, *Tech. Rep. CSC/TM-78/0017*, Comput. Sci. Corp., Greenbelt, Md.

Rasool, S. I., and R. W. Stewart (1971), Results and interpretation of the S-band occultation experiment on Mars and Venus, *J. Atmos. Sci.*, *28*, 869–878, doi:10.1175/1520-0469(1971)028<0869:RAIOTS>2.0.CO;2.

Richmond, A. D. (1987), The ionosphere, in *The Solar Wind and Earth*, edited by S. I. Akasofu and Y. Kamide, pp. 124–140, Terra Sci., Tokyo.

Rishbeth, H., and O. K. Garriott (1969), *Introduction to Ionospheric Physics*, Elsevier, New York.

Rodrigo, R., E. Garcia-Alvarez, M. J. Lopez-Gonzalez, and J. J. Lopez-Moreno (1990), A nonsteady one-dimensional theoretical model of Mars's neutral atmospheric composition between 30 and 200 km, *J. Geophys. Res.*, *95*, 14,795–14,810, doi:10.1029/JB095iB09p14795.

Savich, N. A., and V. A. Samovol (1976), The nighttime ionosphere of Mars from Mars 4 and Mars 5 dual frequency radio occultation measurements, *Space Sci.*, *XVI*, 1009–1010.

Schunk, R. W., and A. F. Nagy (2000), *Ionospheres: Physics, Plasma Physics and Chemistry*, Cambridge Univ. Press, New York.

Seth, S. P., S. A. Haider, and K. I. Oyama (2002), Photoelectron flux and nightglow emission of 5577 and 6300 Å due to solar wind electron precipitation in the Martian atmosphere, *J. Geophys. Res.*, *107*(A10), 1324, doi:10.1029/2001JA000261.

Seth, S. P., U. B. Jayanthi, and S. A. Haider (2006a), Estimation of peak electron density in the upper ionosphere of Mars at high latitude (50°–70°N) using MGS ACC data, *Geophys. Res. Lett.*, *33*, L19204, doi:10.1029/2006GL027064.

Seth, S. P., V. B. Rao, C. M. Espirto Santo, S. A. Haider, and V. R. Choksi (2006b), Zonal variations of peak ionization rates in upper atmosphere of Mars at high latitude using Mars Global Surveyor accelerometer data, *J. Geophys. Res.*, *111*, A09308, doi:10.1029/2006JA011753.

Singhal, R. P., and A. E. S. Green (1981), Spatial aspects of low and medium energy electron degradation in atmospheric oxygen, *J. Geophys. Res.*, *86*, 4776–4785, doi:10.1029/JA086iA06p04776.

Singhal, R. P., and S. A. Haider (1984), Analytical yield spectrum approach to photoelectron fluxes in Earth's atmosphere, *J. Geophys. Res.*, *89*, 6847–6853, doi:10.1029/JA089iA08p06847.

Smith, F. L., and C. Smith (1972), Numerical evaluation of Chapman's grazing incidence integral Ch (χ, χ), *J. Geophys. Res.*, *77*, 3592–3597, doi:10.1029/JA077i019p03592.

Tobiska, W. K., T. Woods, F. Eparvier, R. Viereck, L. Floyd, D. Bouwer, G. Rottman, and O. R. White (2000), The solar 2000 empirical solar irradiance model and forecast tool, *J. Atmos. Sol. Terr. Phys.*, *62*, 1233–1250, doi:10.1016/S1364-6826(00)00070-5.

Torr, D. G., and M. R. Torr (1979), Chemistry of thermosphere and ionosphere, *J. Atmos. Terr. Phys.*, *41*, 797–810, doi:10.1016/0021-9169(79)90126-0.

Vasiliev, M. B., et al. (1975), Preliminary results of dual frequency radio occultation of the Martian ionosphere with the aid of Mars 5 spacecraft in 1974, *Kosm. Issled.*, *13*, 48–51.

Whitten, R. C., I. G. Poppoff, and J. S. Sims (1971), The ionosphere of Mars below 80 km altitude, 1, *Planet. Space Sci.*, *19*, 243–250, doi:10.1016/0032-0633(71)90203-0.

Zbinden, P. A., M. A. Hildago, P. Eberhardt, and J. Geiss (1975), Mass spectrometer measurements of the positive ion composition in the D and E regions of the ionosphere, *Planet. Space Sci.*, *23*, 1621–1642, doi:10.1016/0032-0633(75)90090-2.

Zhang, M. H. G., J. G. Luhmann, and A. J. Kliore (1990), An observational study of the nightside ionosphere of Mars and Venus with radio occultation methods, *J. Geophys. Res.*, *95*, 17,095–17,107, doi:10.1029/JA095iA10p17095.

M. A. Abdu, I. S. Batista, and J. H. Sobral, Department of Aeronomy, Instituto Nacional de Pesquisas Espaciais, Avenue dos Astronauts 1.758, Jd. Granja-CEP 12227-010, São Jose dos Campôs, São Paulo, Brazil.

S. A. Haider, Space and Atmospheric Sciences, Physical Research Laboratory, Navrangpura, Ahmedabad-380009, India. (haider@prl.res.in)

E. Kallio, Finnish Meteorological Institute, Erik Palmenin, aukio1, Post Box 503, Helsinki FIN-00101, Finland.

X. Luan, National Center for Atmospheric Research, 3450 Mitchell Lane, Boulder, CO 80301, USA.

W. C. Maguire, Solar System Exploration Division, NASA Goddard Space Flight Center, Mail Code 693, Greenbelt, MD 20771, USA.

V. Singh, Department of Electronics for Automation, Faculty of Engineering, University of Brescia, Via Branze 38-25123, Brescia, Italy.

M. I. Verigin, Space Research Institute, Russian Academy of Sciences, Profosoyuznaya Street, Moscow, Russia.